Unprecedented Relaxivity Gap in pH-Responsive Fe III -Based MRI Probes

Jeremy Salaam, Thibault Fogeron, Guillaume Pilet, Radu Bolbos, Christophe Bucher, Lhoussain Khrouz, Jens Hasserodt

Unprecedented Relaxivity Gap in pH-Responsive Fe(III)-Based MRI Probes

Jeremy Salaam[a†], Thibault Fogeron[a†], Guillaume Pilet[b], Radu Bolbos[c], Christophe Bucher[a], Lhoussain Khrouz[a] and Jens Hasserodt[a*]

[a] Dr. J. Salaam, Dr. Th. Fogeron, Dr. Ch. Bucher, Dr. Lh. Khrouz, Prof. Dr. J. Hasserodt
Laboratoire de Chimie, UMR CNRS/ENSL 5182
Université de Lyon – ENS de Lyon
46 allee d'Italie, France
E-mail: jens.hasserodt@ens-lyon.fr
[b] Dr. G. Pilet
Laboratoire des Multimatériaux et Interfaces, UMR CNRS/UCBL 5615
Université de Lyon – Université Claude Bernard Lyon 1
DOUA, Villeurbanne, France
[c] Dr. R. Bolbos
Dpt. Animage
CERMEP-Imagerie du Vivant
59 Blvd Pinel, 69677 Bron, France

† These authors have contributed equally to the work.

Abstract: Two mononuclear ferric complexes are reported that respond to a pH change with a 27- and 71-fold jump, respectively, in their capacity to accelerate the longitudinal relaxation rate of water-hydrogen nuclei, and this starting from a negligible base value of only 0.06. This unprecedented performance bodes well for tackling the sensitivity issues hampering the development of Molecular MRI. The two chelates also excel in the fully reversible and fatigue-less nature of this phenomenon. The structural reasons for this performance reside in the macrocyclic nature of the hexa-dentate ligand, as well as the presence of a single pendant arm displaying a five-membered lactam or carbamate which show (perturbed) pK_a values of 3.5 in the context of this N6⇔N5O1 coordination motif.

Converting MRI from a classic imaging modality into a molecular one is a technical as well as a scientific challenge that continues to require tremendous efforts. [1] A chemical solution in the form of a molecular probe able to respond to a biomolecular analyte with a sufficient signal change would have the power to redefine our current view on medical imaging and diagnosis. Academic proposals of probe designs based on the paramagnetic ions Gd(III) or Mn(II) do not yet show enough sensitivity for practical *in vivo* detection of analytes of biomedical interest. In fact, obtaining a satisfactory signal-to-background ratio is not easy to achieve for these metal ions due to the significant relaxivity these probes already generate in their intact state, that is, prior to the encounter of the biomolecular analyte. [2] [3] [4] [5] [6] In addition, the use of gadolinium-based contrast agents (GBCAs) has raised significant health concerns since the early 2000s. [7] [8] [9]

Transition metal complexes, and particularly iron complexes, are now finally beginning to arouse interest as MRI probes[10] [11] for the detection of biomarkers of tissue states such as changing redox potentials, enzyme activity, or changing pH. Prior results from our lab are in line with the observation that these chelates show relaxivity gaps between their un-activated and activated forms that habitually beat the competition. [12] [13] Previously, we had already reported iron-based designs that operate in an irreversible manner as these promise the highest free-energy differences between the un-activated and activated forms and thus a complete response to the bio-analyte. [14] An increase by a factor of 15 (FePyC3A) appears to be the highest gap reported to date, [15] an order of magnitude higher than those reported for probes based on other paramagnetic metal ions.

Here, we describe two pH-responsive, iron(III)-based, molecular probes, **1** and **2**, whose un-activated and activated forms exhibit an unprecedented relaxivity gap. Previously, two pioneering designs of a pH-responsive MRI probe had already been reported: a Gadolinium-based probe designed to serve the classic proton-based MRI modality (1H channel) and showing a relaxivity change of factors of 2 to 4 over a pH range from 5 to 9[16], and a ratiometric lanthanide-based probe operating via a CEST modality.[17] A more recent report describes a pH-responsive FeII-based DOTA complex for 19F and CEST imaging. [18]

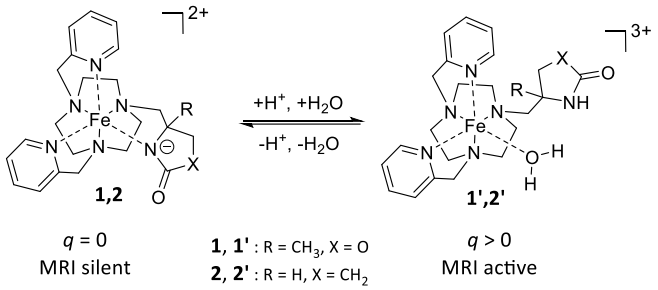

Scheme 1. Activation mechanism of complexes **1** and **2** upon protonation of the coordinated oxazolone type moieties giving rise to an MRI signal in water.

Chelates **1** and **2** were originally intended to be assessed as iron(II) complexes, but they spontaneously oxidize already during synthesis to become ferric chelates. Even though ferric systems cannot adopt a formally spin-silent state (diamagnetism), we will show below that **1** and **2** are capable of unprecedented relaxivity increases upon activation. As desired, the pyrrolidone-based coordinating pendant arms within **1** and **2** reversibly coordinate or de-coordinate the metal center in water in response to changing pH. While the pendant arm in **1** represents a cyclic carbamate, that of **2** constitutes a lactam (Scheme 1).

The cyclic nature of these coordinating sites has been chosen deliberately because this denies the system the ability to coordinate the metal center with any heteroatom on the ring other than nitrogen. As such, either nitrogen coordinates, or water. Free oxazolidinone and pyrrolidone exhibit pK_a's in DMSO of 20.8[19] and 24.2[20], respectively. Importantly, their tautomeric equilibria (iminol vs. carboxamide) are also largely in favor of the carboxamide version. [21] We thus

hypothesized that iron chelates incorporating these heterocycles would only be able to enforce their coordination upon deprotonation to the amidate form. Any protonation to the electroneutral carboxamide form would then automatically result in the heterocycles' de-coordination and thus to a relaxivity increase, hopefully close to physiological pH.

Ferric complexes **1** and **2** were synthesized by alkylation of DPTACN with two tosylated reagents easily accessible from commercial material, followed by complexation with $FeCl_3$ (see SI). Both chelates are purified by RP-HPLC. The last synthetic step, complexation, yielded **1** and **2** in 32% and 23%, respectively. The UV spectra of **1** and **2** in water exhibit an intense *d-d* band at 475 nm and 500 nm, respectively, which is characteristic for ferric complexes (Figures S1 and S2). Their recrystallization in a MeCN/Et_2O mixture furnished purple-colored monocrystals suitable for X-ray diffraction analysis.

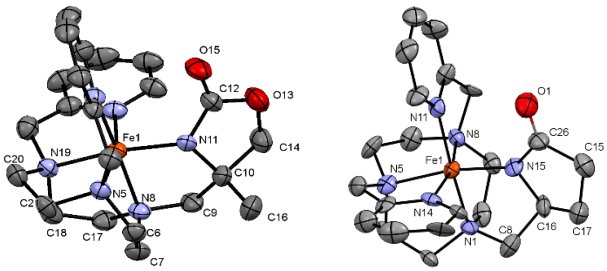

Figure 1. ORTEP representation of X-ray structure analyses[22] of complex **1** (left) and **2** (right). Hydrogens are omitted for clarity.

The resulting structures (Figure 1) [22] showed hexa-coordinate complexes with iron-nitrogen bonds congruent with a low-spin state (ca. 2.00 Å, tables S1 and S2). For complex **1** the C-O bond length of the carbamate group is 1.210 Å, and for complex **2** the same bond for the lactam group is 1.22 Å. These values are in agreement with a C-O double bond as found in the free forms of 2-oxazolidinone and 2-pyrrolidone (1.215 Å[23] and 1.238 Å[24], respectively) while the length of single C-O bonds of the corresponding tautomeric forms should be closer to 1.3 Å. Also, the Fe-N bond of these two moieties is 0.1 Å shorter than the Fe-N bonds of the picolyl pendant arms. It thus has to be concluded that the coordination does not impose an iminolate/imidate form, but rather an amidate, with the negative charge located close to the nitrogen-iron bond. The structure of **1** shows some level of distortion due to the methyl group that requires significant space.

Magnetic moments for both complexes were measured by the Evans method using an NMR spectrometer (Figure S4) in neutral and acidic media. Magnetic moments of 2.12 μ_B (Bohr Magnetons) at pH 7.2, and 2.35 μ_B at pH 0.8 for complex **1**, and 1.87 μ_B at pH 7.0 and 1.94 μ_B at pH 1.2 for complex **2** were determined. The absence of a switch from a low- to a high-spin state due to de-coordination of the pendant arm was also checked by EPR spectroscopy for complex **2** that displayed no signature for a high-spin version of Fe(III), neither in acidic nor in neutral water (Figure S5).

Complex **1** and **2** were submitted to detailed electrochemical analysis in aqueous electrolytes (0.1 M KNO_3) The cyclic voltammogram (CV) of **2** recorded at a glassy carbon working electrode (100 mV/s) displays one reversible wave at $E_{1/2}$ = – 0.11 V (*vs*. ECS) attributed to a one-electron reduction of the iron(III) center (Figure S6). The reversible character of this wave is consistent with the conclusion that the coordination scheme of the iron center does not change significantly over the time scale of this measurement. Conversely, similar measurements with **1** yielded an irreversible reduction wave at E_p = + 0.10 V associated with a re-oxidation signal observed for the reverse scan at 0.42 V (Figure S6). In this case, the irreversible nature of the iron-centered reduction wave is attributed to the poor stability of the electro-generated iron(II) complex which evolves at the CV time scale into a different complex. The observation of a re-oxidation wave at a more positive potential also suggests that the Fe(II) ion is harder to oxidize in the EC product than in the initial complex. Taken together, these data thus lead us to propose that this complex is the reduced version of compound **1'**.

The preferred tautomeric forms of the heterocyclic pendant arms turned out to be those displaying a negative charge on the nitrogen, i.e., the amidate versions. Accordingly, the iron center is stabilized in its ferric state. Hence, our attempt to obtain an iron(II) complex by use of a ferrous salt during synthesis directly led to the ferric complex. Our TACN-based ligands exercise a significant ligand field meant to impose the low-spin state on the corresponding ferrous complexes, and so it does not come as a surprise that the ferric complex is also found in the low-spin state. Indeed, high-spin iron(III) complexes usually exhibit coordination spheres with hard, oxygen-based coordination sites. [25] It is worth noting that the result of a reaction between the ligand and a ferrous salt shows the exact same characteristics as the one with a ferric salt. No de-complexation was observed after spontaneous oxidation, nor any potential loss of stability. This demonstrates the equally good fit of the DPTACN system for iron centers in both oxidation states.

Relaxation time measurements (T_1) of the complexes' aqueous solutions (4 mM) were conducted with a standard NMR spectrometer at 9.4 T (Figure 2). Acid titration from neutral pH (HCl addition) shows progressive reduction of T_1 indicating

the de-coordination of the heterocycle-bearing pendant arm and concurrent access of water to the first coordination sphere. The T_1 values thus reached (0.1 to 0.2 sec) are congruent with a relaxation mechanism involving inner sphere water. As stated above, a non-coordinated lactam (pyrrolidone) exhibits a pK_a of 24.2 in DMSO, that of a cyclic carbamate (oxazolidinone) is found at 12 in water and 20.8 in DMSO. When coordinated to the iron(III) center and considering the strength of the 5-membred chelate ring involved, the pK_a value decreases for both moieties to approximately the same value of 3.5.

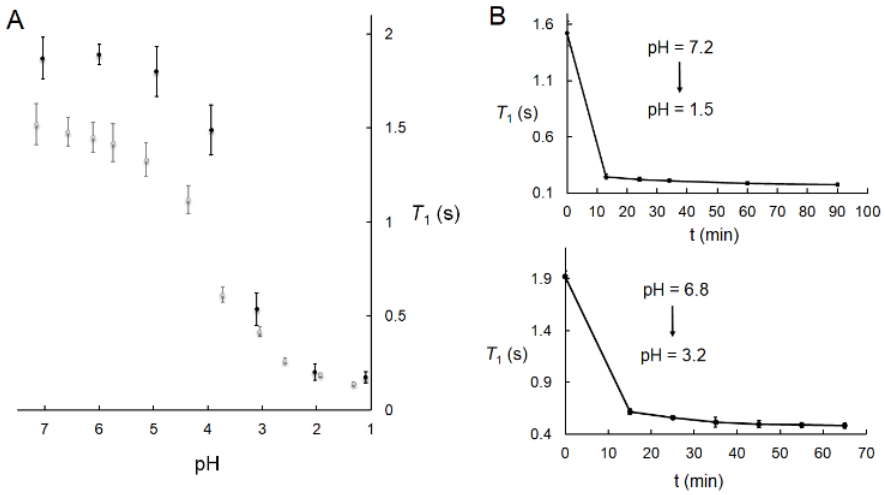

Figure 2. A: T_1 vs pH titration of **1** (grey line) and **2** (dark line) (4 mM) in water monitored by NMR (9.4T); B: Time-dependent response of **1** (top) and **2** (bottom) to acidification.

The initial T_1 plateau at neutral pH was different for both complexes. We investigated the temperature dependency of the activation for one of the complexes (Figure S7), and the T_1 difference is more pronounced at higher temperature (37 °C). This is largely because the T_1 values of the initial, coordinatively closed states differ substantially. Indeed, the temperature dependence of proton relaxation times has been reported previously. [26] This data also illustrates that the pK_a (3.5) is not temperature-dependent.

The kinetics of this pH-dependent response were obtained my measuring T_1 every 10 minutes after an initial acidification. The results show a significant decrease in T_1 during the first 10 minutes (83% and 68% decrease for complex **1** and **2**, respectively), and a further, slower decrease until stabilization at approximately one hour. These kinetics were further investigated with complex **2** by preparing different solutions at different pH and monitoring the T_1 values at larger time points (Figure S8). No further evolution can be detected for the longer waiting times.

That the T_1 values of **1** and **2** at pH 7 do not reach the value for pure water (3.05 sec) should not come as a surprise. We cannot expect the acid-base equilibrium to be of a completely binary nature, i.e., that at pH extremes only one coordination state is populated to a 100 percent. Rather, small proportions of water-coordinated complexes at pH 7 are likely responsible for the observed T_1 values, of course in conjunction with an additional contribution from the outer-sphere influence of the low-spin but paramagnetic metal center. Other contributing factors might be the high concentration used (4 mM, chosen to observe a significant gap in T_1 by titration) and the non-zero spin value of the low-spin ferric center.

The switching capacity of **1** and **2** is remarkably robust. It can endure several cycles of de-coordination/re-coordination without showing any sign of fatigue (Figure 3). The population of the de-coordinated state **1'** and **2'** (reflected by the observed T_1 values) depends on proton concentration and is consistent for every pH value tested.

Subsequently, we determined the relaxivities (at 20°C) for both **1** and **2**, as well as for their activated forms **1'** and **2'**, at the pH values where their respective proportions are the highest in solution, i.e., at pH 7 and 2, respectively. At 7 Tesla (MRI), r_1 for **1** rose from 0.033 to 2.34 mM^{-1} s^{-1} when moving from pH 7 to pH 2. On the other hand, the relaxivity of chelate **2** increased from r_1 = 0.06 to 1.60 $mM^{-1}s^{-1}$. Thus, at 7 T, their relaxivities soar by factors of 71 (**1**) and 27 (**2**) as a response to a pH change from 7 to 2 (Table 1). This behavior is reflected in the hypersignal differences generated by an MRI instrument (7 Tesla) for aqueous solutions of **1** and **2** at pH 2 vs. pH 7 (Figure 4).

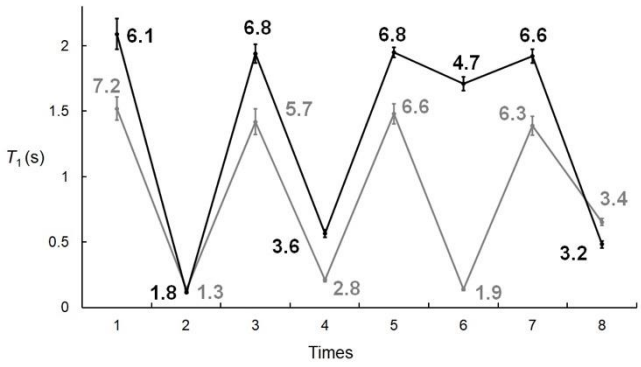

Figure 3. Switching capacity of complex **1** (grey line) and **2** (dark line).

Table 1. r_1 values ($mM^{-1}\ s^{-1}$) obtained at 20°C in pure water at pH 7 (**1** and **2**) and pH 2 (1' and 2'), and at 7 T MRI field strength (extracted from phantom images).

Compound	**1**	**1'**	**2**	**2'**
r_1 ($mM^{-1}\ s^{-1}$)	0.033 ± 0.001	2.34 ± 0.04	0.06 ± 0.0005	1.60 ± 0.28

The absence of any notable relaxivity at pH 7 for both coordinatively closed complexes is congruent with the same observations in a previous report on low-spin iron(III) complexes in aqueous solution whose first coordination sphere is fully occupied by their ligand.[27] On the opposite side, the relaxivity for the activated form is in the high region of values for iron-based contrast agents and does well compete with values reported for GBCAs. Both of

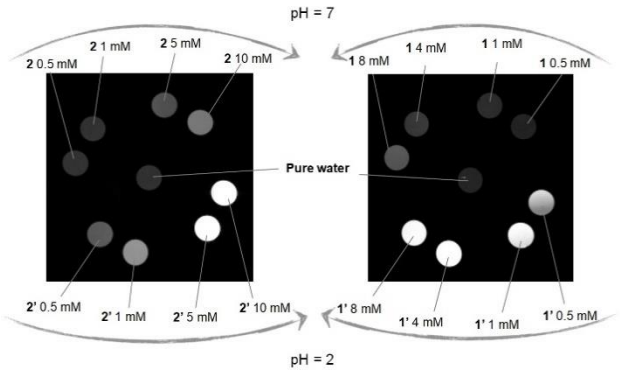

Figure 4. MRI phantom images of aqueous solutions of **1** (left panel) and **2** (right) at pH 7 (upper sample tubes) and 2 (lower).

these two features are equally important, as they ensure a low background signal for the un-activated form of the probe and a sizeable MRI signal after activation, i.e., the desired significant signal gap for a responsive probe as emphasized in the introduction.

Two key design features are likely responsible for the unprecedented performance described above: (1) use of the DPTACN macrocycle that ensures high water stability, the adoption of resolutely low-spin states for both forms of the probes and a facile approach of water molecules, and (2) heterocycle-bearing, pendant arms which ensure the adoption of a single coordination state at opposite sides of a given pH interval. Also, these heterocycles might contribute to the high observed relaxivities for the activated forms.

As described above, the low-spin state of the ferric centers does not change with a water molecule replacing the coordinated heterocycle, a phenomenon not observed with ferrous centers. It is notable that this does not compromise the observation of a high signal gap upon activation of the ferric versions. Finally, we also measured the relaxivity of the activated version with an NMR spectrometer (9.4 T). The observed values rose by a factor of 1.3 for both complexes when going from 7 T to 9.4 T (Figures S9, S11 and table S4). This agrees with a previous report where an iron-based chelate

shows increased relaxivity with increasing magnetic field[28], while Gadolinium- and Mn-based contrast agents see a systematic decrease. [29]

Past reports of analyte-responsive Gadolinium-based small-molecule contrast agents spoke of relaxivity changes of 20, 40, 75, even 100 *percent*.[30] In all these cases, their unreacted versions were decent contrast agents, sporting relaxivities anywhere between 2 and 4 mM^{-1} s^{-1}, in other words also giving off a sizeable signal in the absence of the analyte. The same holds true for more recent materials-based, pH-responsive contrast agents still employing Gadolinium, even though a relaxivity change by a factor of 4 was achieved.[31] However, a satisfying performance solely regarding the criterion of relaxivity change is not sufficient for a viable solution. Many other parameters have to be taken into account, above all stability (robustness).[32] Recent work reported a relaxivity increase by a factor of 15 using an iron-based approach. [15] Such reports currently arouse increasing interest in the field. Our proposal to overcome the sensitivity issue with the concept of an iron-based molecular probe date back to 2005[33] and 2008. [12]
The system described here exhibits heretofore unknown relaxivity increases by factors of 27 and 71, respectively. The un-activated version is essentially MRI-silent. This unprecedented signal gap competes well with the performance of ^{19}F MRI or CEST-MRI probes but outperforms them in view of the vitally important advantages associated with the use of ^{1}H MRI. The system's robust performance encourages further development into a probe responding to the presence of biomolecular analytes at physiological pH.

Acknowledgements

We thank Dr. Pascal Fries, CEA Grenoble, for the measurement of the NMRD profiles.

Keywords: Molecular MRI • pH-responsive molecular probes • iron(III) chelates • relaxivity • detection sensitivity

References

[1] I. K. Cho, S. Wang, H. Mao, A. W. Chan, *Am J Nucl Med Mol Imaging* **2016**, *6*, 234–261.

[2] J. L. Major, T. J. Meade, *Acc. Chem. Res.* **2009**, *42*, 893–903.

[3] E. L. Que, C. J. Chang, *Chem. Soc. Rev.* **2010**, *39*, 51–60.

[4] G.-L. Davies, I. Kramberger, J. J. Davis, *Chem. Commun. (Camb.)* **2013**, *49*, 9704–9721.

[5] J. Wahsner, E. M. Gale, A. Rodríguez-Rodríguez, P. Caravan, *Chem. Rev.* **2019**, *119*, 957–1057.

[6] S. M. Pinto, V. Tomé, M. J. F. Calvete, M. M. C. A. Castro, É. Tóth, C. F. G. C. Geraldes, *Coordination Chemistry Reviews* **2019**, *390*, 1–31.

[7] J. Lunyera, D. Mohottige, A.-S. Alexopoulos, H. Campbell, C. B. Cameron, N. Sagalla, T. J. Amrhein, M. J. Crowley, J. R. Dietch, A. M. Gordon, et al., *Annals of Internal Medicine* **2020**, *173*, 110–119.

[8] M. N. Rozenfeld, D. J. Podberesky, *Pediatric Radiology* **2018**, *48*, 1188–1196.

[9] J. Ramalho, R. C. Semelka, M. Ramalho, R. H. Nunes, M. AlObaidy, M. Castillo, *AJNR Am J Neuroradiol* **2016**, *37*, 1192–1198.

[10] J. Salaam, M. Rivat, T. Fogeron, J. Hasserodt, *Analysis & Sensing* **2021**, *1*, 11–29.

[11] A. Gupta, P. Caravan, W. S. Price, C. Platas-Iglesias, E. M. Gale, *Inorg. Chem.* **2020**, *59*, 6648–6678.

[12] V. Stavila, M. Allali, L. Canaple, Y. Stortz, C. Franc, P. Maurin, O. Beuf, O. Dufay, J. Samarut, M. Janier, et al., *New J. Chem.* **2008**, *32*, 428–435.

[13] F. Touti, A. K. Singh, P. Maurin, L. Canaple, O. Beuf, J. Samarut, J. Hasserodt, *J. Med. Chem.* **2011**, *54*, 4274–4278.

[14] H. Wang, M. B. Cleary, L. C. Lewis, J. W. Bacon, P. Caravan, H. S. Shafaat, E. M. Gale, *Angew. Chem. Int. Ed. Engl.* **2022**, *61*, e202114019.

[15] F. Touti, P. Maurin, L. Canaple, O. Beuf, J. Hasserodt, *Inorg. Chem.* **2012**, *51*, 31–33.

[16] F. G. Bordwell, H. E. Fried, *J. Org. Chem.* **1991**, *56*, 4218–4223.

[17] F. G. Bordwell, *Acc. Chem. Res.* **1988**, *21*, 456–463.

[18] M. M. Karelson, A. R. Katritzky, M. Szafran, M. C. Zerner, *J. Chem. Soc., Perkin Trans. 2* **1990**, 195–201.

[19] M. Fimberger, K. P. Luef, C. Payerl, R. C. Fischer, F. Stelzer, M. Kállay, F. Wiesbrock, *Materials (Basel)* **2015**, *8*, 5385–5397.

[20] R. Goddard, O. Heinemann, C. Krüger, I. Magdó, F. Mark, K. Schaffner, IUCr, *Acta Crystallogr Sect C Cryst Struct Commun* **1998**, *54*, 501–504.

[21] E. M. Snyder, D. Asik, S. M. Abozeid, A. Burgio, G. Bateman, S. G. Turowski, J. A. Spernyak, J. R. Morrow, *Angew. Chem. Int. Ed. Engl.* **2020**, *59*, 2414–2419.

[22] T. R. Nelson, S. M. Tung, *Magnetic Resonance Imaging* **1987**, *5*, 189–199.

[23] P. B. Tsitovich, F. Gendron, A. Y. Nazarenko, B. N. Livesay, A. P. Lopez, M. P. Shores, J. Autschbach, J. R. Morrow, *Inorg. Chem.* **2018**, *57*, 8364–8374.

[24] D. Asik, S. M. Abozeid, S. G. Turowski, J. A. Spernyak, J. R. Morrow, *Inorg. Chem.* **2021**, *60*, 8651–8664.

[25] Z. Baranyai, F. Carniato, A. Nucera, D. Horváth, L. Tei, C. Platas-Iglesias, M. Botta, *Chem. Sci.* **2021**, *12*, 11138–11145.

[26] C.-Y. Cao, Y.-Y. Shen, J.-D. Wang, L. Li, G.-L. Liang, *Sci Rep* **2013**, *3*, 1–9.

[27] W. Zhang, J. A. Peters, F. Mayer, L. Helm, K. Djanashvili, *J. Phys. Chem. C* **2015**, *119*, 5080–5089.

[28] J. Hasserodt, J. L. Kolanowski, F. Touti, *Angew. Chem.-Int. Edit.* **2014**, *53*, 60–73.

[29] J. Hasserodt, *Contrast Agents for Magnetic Resonance Imaging*, **2005**, WO2005094903A2.